CrossMark

ORIGINAL PAPER

Development of proton conducting biopolymer membrane based on agar–agar for fuel cell

G. Boopathi[1,2] · S. Pugalendhi[1] · S . Selvasekarapandian[2] · M. Premalatha[2] ·
S. Monisha[2] · G. Aristatil[3]

Abstract A proton-conducting polymer electrolyte based on agar and ammonium nitrate (NH_4NO_3) has been prepared through solution casting technique. The prepared polymer electrolytes were characterized by impedance spectroscopy, X-ray diffraction, and Fourier transform infra-red spectroscopy. Impedance analysis shows that sample with 60 wt.% NH_4NO_3 has the highest ionic conductivity of 6.57×10^{-4} S cm^{-1} at room temperature. As a function of temperature, the ionic conductivity exhibits an Arrhenius behaviour increasing from 6.57×10^{-4} S cm^{-1} at room temperature to 1.09×10^{-3} S cm^{-1} at 70 °C. Transport parameters of the samples were calculated using Wagner's polarization method and thus shows that the increase in conductivity is due to the increase in the number of mobile ions. Fuel cell has been constructed with the highest proton conductivity polymer 40agar/60NH_4NO_3 and the open circuit voltage is found to be 558 mV.

Keywords Biopolymer · agar-agar · AC-impedance spectroscopy · Fuel cell

Introduction

The present concern on the depletion of fossil fuel resources and the environmental issues caused by it gave rise to fuel cell technologies which have received much attention in recent years due to their high efficiencies and low emissions. The reason that Nafion® is being the principal material used as a polymeric electrolyte is because of its excellent chemical and mechanical stabilities, and high proton conductivity. However, Nafion® and similar perfluorinated polymers have relevant drawbacks, including a high methanol permeability, a decrease in conductivity at high temperatures ($T = 80$ °C) and an elevated cost [1, 2].

In this context, studies have accentuated the development of solid polymer electrolytes (SPEs) as they offer some advantages over liquid electrolytes, such as higher temperatures of operation, no flowing and corrosion after damage and ease of application to fuel cell and other electrochemical devices. Synthetic polymers have been widely used as polymer host in SPEs, but they are non-biodegradable and toxic which can cause environmental issues [3]. Hence, it is imperative to develop the biopolymer electrolytes by using natural polymer, which has gained more and more attention, owing to their abundance in nature, low cost, friendliness to the environment and potential as substitute for some petrochemicals [4]. Chitosan, starch, pectin, agar, methyl cellulose and cellulose acetate are natural polymers, which have been proposed by researchers to develop SBP electrolytes [5, 6].

agar which is commonly known as agar-agar, typically a strong gelling polysaccharide derived from red seaweeds and is characterized by its chemical repeat units of 3–6, anhydro L-galactose [7]. It is a biodegradable, hydrophilic, cheap, non-toxic and chemically stable natural polymer. Similar to starch, agar is a heterogeneous mixture of two polysaccharides: agaropectin and agarose. Both polymers share the same galactose-based backbone, but agaropectin is heavily modified with acidic side groups such as sulphate and pyruvate. In contrast, agarose is the low-sulphate, neutral gelling fraction of agar [8].

✉ S . Selvasekarapandian
  sekarapandian@rediffmail.com

1 Department of Bioenergy, Tamil Nadu Agricultural University, Coimbatore, Tamil Nadu 641003, India

2 Materials Research Center, Coimbatore, Tamil Nadu 641045, India

3 Ingsman Energy and Fuel cell Organization Pvt Ltd., Chennai, Tamil Nadu 600096, India

Springer

There has been only a few number of studies using agar-based electrolytes for the application in electrochemical devices, among which most of them are gel polymer electrolytes (GPEs). Moon et al. developed a biodegradable gel electrolyte based on NaCl-agarose gel for use in flexible super capacitors. They found that these gel electrolytes enabled the super capacitor to have a high specific capacitance of 286.9 F g^{-1} [9]. Koh et al. have studied Bacto agar-based gel polymer electrolyte doped with sodium iodide and iodine [10]. Singh et al. have studied gel polymer electrolyte based on agarose polymer matrix doped with potassium iodide for dye-sensitized solar cell applications and found that the maximum ionic conductivity value of 9.02×10^{-3} S cm^{-1} for the film with 60 % agarose and 40 % KI [11]. The same authors have reported a study of biopolymer based on Sago-palm to develop solid polymer electrolyte for dye-sensitized solar cells [12].

Raphael et al. prepared a polymer electrolyte based on agar and acetic acid and reported the ionic conductivity which was found to be 1.1×10^{-4} S cm^{-1} [8]. Alias and Mohamed prepared gel polymer electrolytes using agar as host polymer with dopants NH_4I and I_2. They found the maximum conductivity value as 2.64×10^{-4} S cm^{-1} [13]. The present work aims to develop a novel proton-conducting biopolymer electrolyte with agar as a host polymer while ammonium nitrate (NH_4NO_3) was chosen as the ionic dopant. The prepared SBP electrolytes were characterized by Fourier transform infrared (FTIR), X-ray diffraction (XRD), electrical impedance spectroscopy (EIS) and transference number measurement (TNM). Finally, using these complex polymer electrolyte agar/NH_4NO_3 with high ionic conductivity, single proton exchange membrane (PEM) fuel cell was constructed and its open circuit voltage was measured.

Materials and methods

Preparation of electrolyte

In this study, the polymer agar-agar (Colloids Impex Pvt. Ltd) and ammonium nitrate (Merck) are used as the raw materials. The solvent used was distilled water and the polymer electrolytes were prepared using solution casting technique. Since agar-agar is not readily soluble in normal water, it is dissolved in boiling water and stirred continuously in a magnetic stirrer until a clear solution is obtained. Then, different molar ratios of ammonium nitrate (10, 20, 30, 40, 50, 60 and 70 %) were added and the mixture was stirred for another 1 h to obtain a transparent solution. The solution was then casted into glass Petri dishes and transferred to hot air oven where it was dried at 45 °C overnight. The obtained film was used for the subsequent experimentation.

Characterization techniques

X-ray diffraction

XRD measurements were performed using Rigaku Ultima IV Multipurpose X-ray diffraction system with the Cu-ka radiation range of diffraction angle 2θ from 10° to 80° at a rate of 2° min^{-1} to determine the extent of crystalline/amorphous phase present in the electrolytes.

Fourier transform infrared

FTIR analyses were performed using the SHIMADZU-IR Affinity-1 spectrophotometer in the range of 4000–500 cm^{-1}. The analyses were carried out to observe any changes and shifts of the characteristic band due to the chemical interaction of agar-agar with the ammonium salts.

Impedance spectroscopy

The measurement of the bulk resistance (R$_b$) of the sample was carried out by alternating current (AC) impedance measurement using HIOKI 3532 LCR meter in the frequency ranging from 42 Hz to 1 MHz. The sample was sandwiched between two aluminium blocking electrodes with a contact area of 2.0 cm^2. The bulk resistance (R$_b$) was determined from the equivalent circuit analysis by using EQ software [14, 15]. The conductivity values (σ) of electrolyte were calculated based on the equation

$$\sigma = l/R_b A \qquad (1)$$

where l is the thickness, R$_b$ is the bulk resistance and A is the contact area of the electrolyte film.
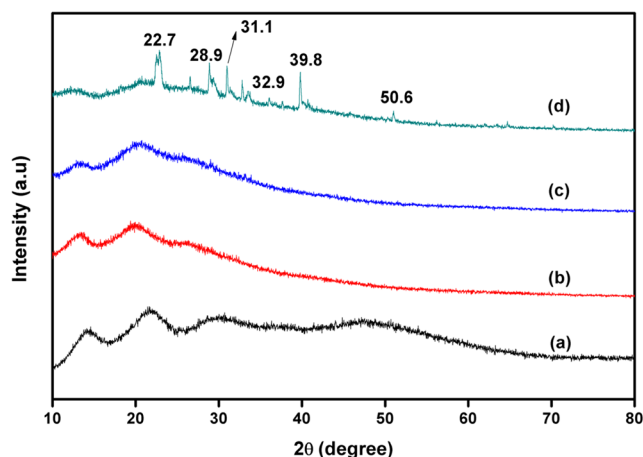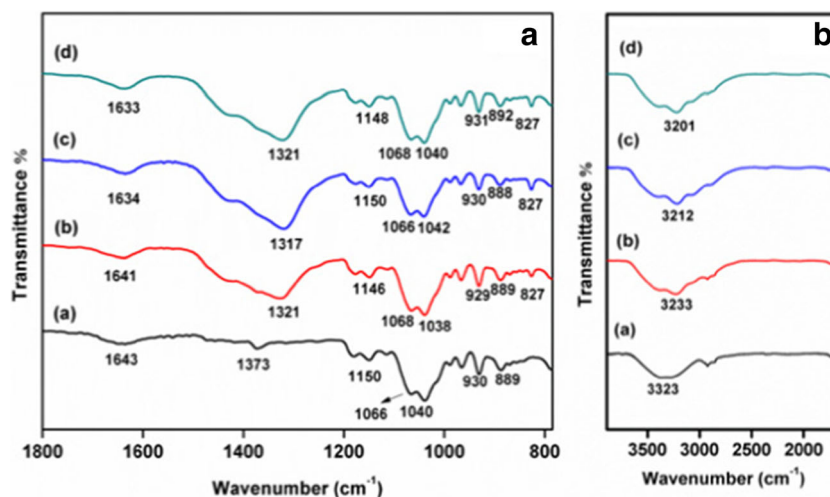

Fig. 1 XRD profile of **a** pure agar, **b** 50agar/50NH$_4$NO$_3$, **c** 40agar/60NH$_4$NO$_3$, **d** 30agar/70NH$_4$NO$_3$ BPEs

Fig. 2 **a** FTIR spectra of *a* pure
agar, *b* 50agar/50NH$_4$NO$_3$, *c*
40agar/60NH$_4$NO$_3$, *d* 30agar/
70NH$_4$NO$_3$ BPEs. **b** FTIR spectra
of hydroxyl group (OH) *a* pure
agar, *b* 50agar/50NH$_4$NO$_3$, *c*
40agar/60NH$_4$NO$_3$, *d* 30agar/
70NH$_4$NO$_3$ BPEs

Results and discussion

X-ray diffraction analysis

The effect of inclusion of NH$_4$NO$_3$ in the biopolymer agar-
agar can be studied using XRD analysis. Figure 1 depicts
the XRD diffractograms of pure agar and complex of agar-
agar and NH$_4$NO$_3$ (50agar/50NH$_4$NO$_3$, 40agar/
60NH$_4$NO$_3$, 30agar/70NH$_4$NO$_3$). The broad peaks for
undoped agar electrolyte are present at $2\theta = 13.92°$,
21.5°, 29.89° and 48°. The XRD patterns indicate that
the broadness of the peak increases with increase in salt
concentration which reveals that as ion concentration in the
electrolyte increases, amorphousness is also increased
[16]. The peak intensity was observed to be minimum for
the polymer complex 40agar/60NH$_4$NO$_3$, indicating that
the electrolyte has the highest amorphous content which
is consistent with the conductivity result. Since ions are
preferably mobile in the amorphous phase, these results
explain the increasing conductivity value with increasing
NH$_4$NO$_3$ content up to 60 wt.% [17]. This amorphous na-
ture in the polymer complex can be interpreted in terms of
Hodge et al.'s criterion which has established a correlation
between the height of the peak and degree of crystallinity.

The peak corresponding to the NH$_4$NO$_3$ salt (JCPDS
85–1093) was absent up to 40agar/60NH$_4$NO$_3$ and was

observed in the polymer complex 30agar/70NH$_4$NO$_3$
which is represented in Fig. 1d. Presence of these peaks
indicates that the host polymer could no longer solvate the
salt. Hence, a considerable amount of salt is not entrapped
in the host polymer and deposited on the surface, which
eventually leads to the decrease in the number of mobile
ions in the sample and to decrease in the conductivity of
the electrolytes [18].

The XRD results also supports the impedance analysis.
The change in bulk resistance pattern of the electrolytes
can be attributed to structural changes in the polymer
electrolytes [19, 20]. As the NH$_4$NO$_3$ salt concentration
increases, the amorphousness of the pure agar tends to
increase which results in the greater ionic diffusivity and
high ionic conductivity compared to the pure agar elec-
trolytes. The excessive addition of salts causes polymer
chain shrinkage and phase disengagement between poly-
mer matrix and the electrolyte which in turn causes many
ions to remain in the electrolyte and the conductivity re-
mains stable or to decrease slightly [21].

Fourier transform infrared analysis

Infrared analysis is a powerful tool to investigate the com-
plex formation and local structural changes in the polymer
electrolyte matrices. Figure 2a, b elucidates the FTIR

Table 1 FTIR assignments of the calculated and observed vibrational frequencies of agar/ NH$_4$NO$_3$ BPEs

Pure agar experimental (cm^{-1})	50agar/50NH$_4$NO$_3$ (cm^{-1})	40agar/60NH$_4$NO$_3$ (cm^{-1})	30agar/70NH$_4$NO$_3$ (cm^{-1})	Assignments
930	929	930	931	3,6-anhydro-galactose
1066	1068	1066	1068	C–O–C stretching
1373	1321	1317	1321	CH$_2$ in plane bending
1643	1641	1634	1633	Amine (NH) and acetone (CO) group
3323	3233	3212	3201	OH stretching
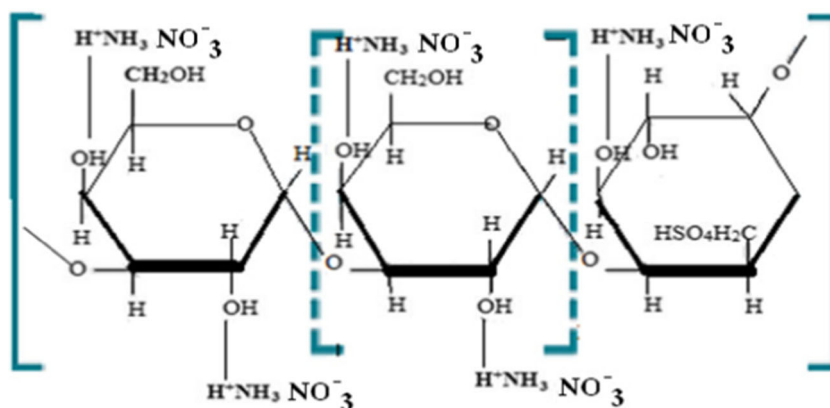
spectrum of biopolymer electrolytes (BPEs) at various concentrations of NH$_4$NO$_3$. The most important vibrational modes and wavenumbers exhibited by pure agar are 3,6-anhydro-galactose at 930 and two humps at 1066 and 1040 cm^{-1} [22], ester sulphate link vibration at 1373 cm^{-1} [23] and amine (NH), acetone groups (CO) at 1643 cm^{-1}, [24] respectively. The band around 1150 and 889 cm^{-1} has been due to typical sulphate ester link [25]. The FTIR peak positions and assignments for pure agar are supported by literature [24, 26, 27]. The observed FTIR peak position and intensity (930, 1066, 1373 and 1643 cm^{-1}) have been shifted due to the addition of 50, 60 and 70 mol% of NH$_4$NO$_3$ with agar. FTIR absorption band position, shifting and assignments of all prepared BPEs are listed in Table 1.

From Fig. 2b, the broad band at 3323 cm^{-1} in pure agar has been ascribed to intermolecular hydrogen bonding and hydroxyl group (OH) stretching, which is not due to water content. The shift in the wavenumber (3323 to 3201 cm^{-1}) of OH group in the complexes gives the strong indication of interaction between dopant salt

NH$_4$NO$_3$ and host polymer agar. Previous work by Ramesh et al. also observed that the hydroxyl band of corn starch has shifted from 3402 to 3415 cm^{-1} [28]. The proton conduction in BPE film has been occurred by lone pair migration or vehicular mechanism. One of the loosely bound protons of NH$_4^+$ ion serves as a conduction species in agar/NH$_4$NO$_3$ BPEs, which has been proved in many literatures [29, 30]. The salt NH$_4$NO$_3$ has strong tendency to denote the proton, and thus it is suggested as the main point of interaction with polar groups in agar matrix. Hence, the polar group or active sites in the agar matrix would be the interesting coordinate sites for lone pair proton, which formed with oxygen that carries available lone pair electron in this group [31].

Referring to Fig. 2a, the appearance of new peak at 827 cm^{-1} corresponds to C–C stretching and affected band at 1373 cm^{-1} have been due to the addition of NH$_4$NO$_3$ [32]. Possible interaction between agar and salt NH$_4$NO$_3$ has been shown in Scheme 1. The addition of NH$_4$NO$_3$ promoted the ion dissociation so that more ions interact with the polymer host at the hydroxyl group. This

Fig. 3 a Cole–Cole plot for pure agar. b Cole–Cole plot of a 90agar/10NH$_4$NO$_3$, b 80agar/20NH$_4$NO$_3$, c 70agar/30NH$_4$NO$_3$, d 60agar/40NH$_4$NO$_3$, e 50agar/50NH$_4$NO$_3$, f 40agar/60NH$_4$NO$_3$, g 30agar/70NH$_4$NO$_3$ BPEs. c Cole–Cole plot for highest conductivity BPE at different temperature
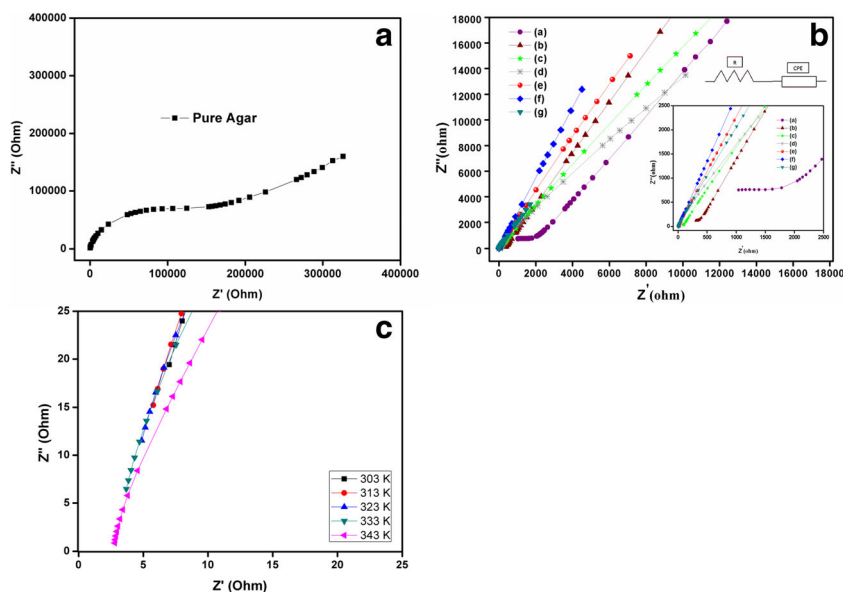
Table 2 EIS parameters

Polymer composition (mol %)	R, Ω	CPE, μF
Pure agar	1.69×10^5	8.612×10^{-4}
90agar/10NH$_4$NO$_3$	1.57×10^3	0.183
80agar/20NH$_4$NO$_3$	258	0.325
70agar/30NH$_4$NO$_3$	21.4	1.41
60agar/40NH$_4$NO$_3$	18.9	0.968
50agar/50NH$_4$NO$_3$	8.62	1.43
40agar/60NH$_4$NO$_3$	2.94	1.31
30agar/70NH$_4$NO$_3$	4.4	0.949

leads to the development of the electrolyte system. Thus, FTIR analysis proves the complex formation between polymer agar and NH$_4$NO$_3$ BPEs.

AC impedance spectroscopy

Cole–Cole plot

Figure 3a shows a part of depressed semicircle which is for the pure agar electrolyte. Figure 3b shows the Cole–Cole plot for all the polymer complexes of agar/NH$_4$NO$_3$ at room temperature. The semicircle can be represented by a parallel combination of capacitor, which is mainly due to immobile polymer chain [33]. In this study, as the salt concentration begins to increase, the semicircle in the plots tends to lessen and finally leaves only a low-frequency spike. This infers that only resistive component exists in the polymer electrolyte, which is due to the mobile ions in the polymer matrix [34]. The equivalent circuit is shown in Fig. 3b. Electrochemical impedance spectroscopy (EIS) parameters were obtained from the Cole–Cole plot by using the EQ software, which are listed in Table 2. From the table, the resistance value of pure agar was obtained as $1.69 \times 10^5 \Omega$, whereas for 10–70 mol% of NH$_4$NO$_3$ doped with agar polymer electrolyte, the value of resistance was decreased from 1570 to 4.4 Ω. The constant phase element (CPE) value for pure CA was

obtained as 8.612×10^{-4} μF. The NH$_4$NO$_3$ doped with agar polymer electrolyte have CPE values in the range of 0.184–1.43 μF. The highest conductivity polymer electrolyte 40agar/60NH$_4$NO$_3$ has R$_b$ = 2.94 Ω and CPE = 1.31 μF.

Cole–Cole plot for the highest conductivity polymer complex 40agar/60NH$_4$NO$_3$ at various temperatures is shown in Fig. 3c. The plot consists of low-frequency spike which is due to the blocking electrodes. As the temperature increases, the resistance of the electrolyte is found to decrease. This may be due to the increase in mobility of charge carriers that enhances the conductivity. It is seen from Table 2 that the conductivity of all polymer electrolytes increases with increasing temperature.

Conductivity analysis

There are many factors that influence the ionic conductivity such as ionic-conducting charge species concentration, cationic- or anionic-type charge carriers, the mobility of charge carriers and temperature [35]. The ionic conductivity values calculated using Eq. 1 for various compositions of agar electrolytes with ammonium nitrate salt are depicted in Table 3. At ambient temperature, the maximum value of ionic conductivity is found to be 6.57×10^{-4} S cm^{-1} for 40agar/60NH$_4$NO$_3$ polymer complex whereas the conductivity of pure agar electrolyte is 1.98×10^{-8} S cm^{-1}. This higher ionic conductivity of 40agar/60NH$_4$NO$_3$ may be due to the transition from semi-crystalline phase to amorphous and increase in charge carrier concentration [36].

The conductivity of an electrolyte is much affected by the number density of charge carriers [6]. The increase of mobile charge carriers in polymer electrolyte was due to the fact that the salt and polymer host have interacted, which led to the high dispersion of H$^+$ that resulted in the increase of conductivity. On addition of more than 60 wt.% NH$_4$NO$_3$, the conductivity starts to decrease which may have attributed to the formation of ion aggregates. The existence of salt aggregates in the electrolytes is because of the re-association of anions and cations. When too much salt is added to the polymer host, the ions

Table 3 Ionic conductivity and activation energy values for agar/NH$_4$NO$_3$ polymer electrolyte for different temperature

Polymer composition (mol %)	Ionic conductivity (S cm^{-1})					Activation energy at room temperature (eV)
	303 K	313 K	323 K	333 K	343 K	
Pure agar (100 %)	1.98×10^{-8}	3.31×10^{-8}	6.08×10^{-8}	1.06×10^{-7}	2.08×10^{-7}	0.53
90agar/10NH$_4$NO$_3$	4.98×10^{-6}	1.09×10^{-5}	1.67×10^{-5}	2.74×10^{-5}	4.78×10^{-5}	0.49
80agar/20NH$_4$NO$_3$	1.67×10^{-5}	2.42×10^{-5}	3.79×10^{-5}	6.51×10^{-5}	1.19×10^{-4}	0.44
70agar/30NH$_4$NO$_3$	4.16×10^{-5}	5.78×10^{-5}	8.65×10^{-5}	1.28×10^{-4}	1.86×10^{-4}	0.34
60agar/40NH$_4$NO$_3$	9.93×10^{-5}	1.35×10^{-4}	2.13×10^{-4}	3.17×10^{-4}	4.66×10^{-4}	0.35
50agar/50NH$_4$NO$_3$	1.89×10^{-4}	2.35×10^{-4}	3.41×10^{-4}	5.63×10^{-4}	7.87×10^{-4}	0.33
40agar/60NH$_4$NO$_3$	6.57×10^{-4}	6.68×10^{-4}	8.90×10^{-4}	9.06×10^{-4}	1.09×10^{-3}	0.12
30agar/70NH$_4$NO$_3$	4.51×10^{-4}	6.26×10^{-4}	7.30×10^{-4}	7.52×10^{-4}	7.66×10^{-4}	0.13
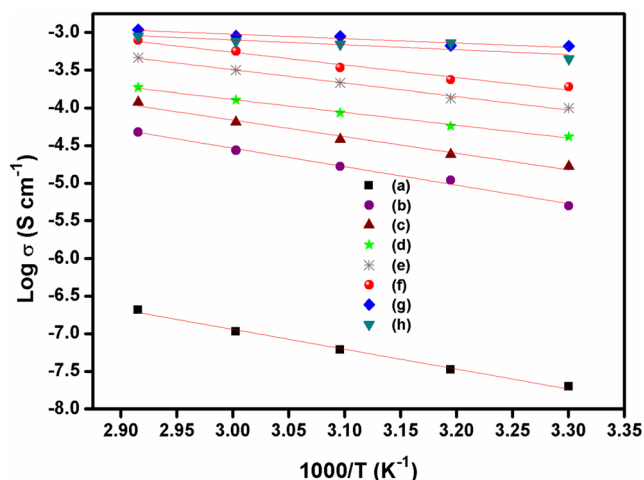
Fig. 4 Arrhenius plot for *a* 90agar/10NH$_4$NO$_3$, *b* 80agar/20NH$_4$NO$_3$, *c* 70agar/30NH$_4$NO$_3$, *d* 60agar/40NH$_4$NO$_3$ *e* 50agar/50NH$_4$NO$_3$, *f* 40agar/60NH$_4$NO$_3$, *g* 30agar/70NH$_4$NO$_3$ BPEs

and cations can be close to each other so that they can form salt aggregates which will hinder other free ions to move as well as reduce the number of density of free mobile ions, hence decreasing the conductivity. The conductivity reported in the literature is only for agar-based gel polymer electrolytes. Koh et al. and Singh et al. have studied GPE based on agar with sodium iodide and agar with potassium iodide respectively. Their conductivity value (of the order 10^{-3} S cm^{-1}) is not related with the proton conductivity. No one has reported proton conductivity of agar-based solid polymer electrolytes except Raphael et al., who studied the proton conductivity of solid polymer electrolyte based on agar and acetic acid, and the value is 1.1×10^{-4} S cm^{-1}, which is less than that of our proton conductivity value (6.57×10^{-4} S cm^{-1}).

Temperature-dependent conductivity

The temperature dependence of ionic conductivity measurements for the polymer complex agar/NH$_4$NO$_3$ was taken in
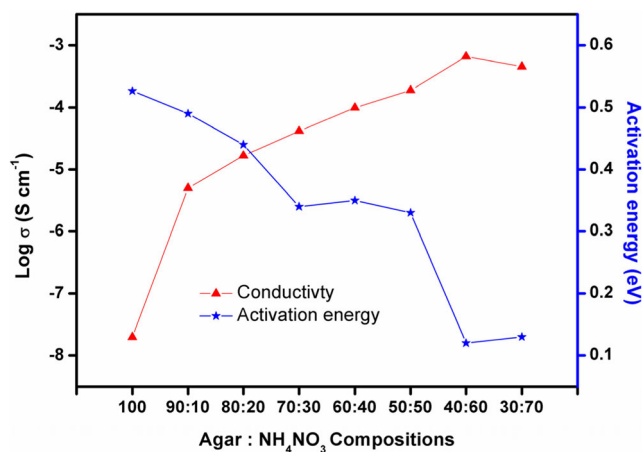
order to analyse the mechanism of ionic conduction in polymer electrolytes. The measurements were taken in the temperature range of 303–343 K. Figure 4 shows the conductivity plot between log (σ) and 1000/T, which indicates that the conductivity increases with increase in temperature for all the compositions. The linear variation of this plot suggests an Arrhenius-type thermal-activated process. Linear relations are observed in all the samples indicating that there is no phase transition in the polymer by the addition of NH$_4$NO$_3$. The conductivity can be measured by

$$\sigma = \sigma_0 \exp(-E_a/kT) \qquad (2)$$

where σ_0 is the pre-exponential factor, Ea is the activation energy, and K is the Boltzmann constant. Activation energy (Ea) values were calculated for all prepared polymer electrolytes by the linear fitting of Arrhenius plots which is given in Table 3. Figure 5 relates the conductivity and activation energy for all the polymer complex electrolytes. This indicates that the activation energy value decreases with the increase in salt concentration. This is in agreement with the fact that the number of ions in the polymer electrolyte increases with increasing in NH$_4$NO$_3$ concentration, and the energy barrier for the proton transport decreases, leading to a decrease in the activation energy [37].

Conduction spectra

The variation of ac conductivity with frequency for different compositions of agar/NH$_4$NO$_3$ polymer electrolytes is shown in Fig. 6. In general, the conductance spectra can be divided into three regions, which are low-frequency dispersion region, frequency-independent plateau region and high-frequency region. The low frequency dispersion region represents the space charge polarization at the blocking electrodes. The frequency-independent plateau region on the log σ (y-axis)
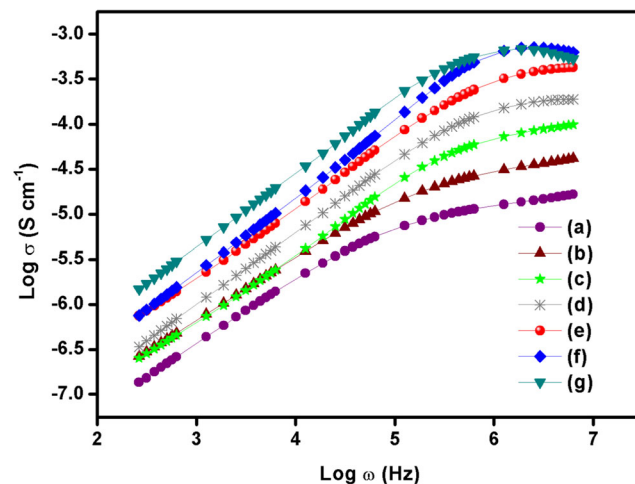

Fig. 5 Variation of conductivity and activation energy as a function of salt concentration NH$_4$NO$_3$

Fig. 6 Conductance spectra for *a* 90agar/10NH$_4$NO$_3$, *b* 80agar/20NH$_4$NO$_3$, *c* 70agar/30NH$_4$NO$_3$, *d* 60agar/40NH$_4$NO$_3$ *e* 50agar/50NH$_4$NO$_3$, *f* 40agar/60NH$_4$NO$_3$, *g* 30agar/70NH$_4$NO$_3$ BPEs

Fig. 7 **a**, **b** Frequency dependence of ε' and ε'' of *a* 90agar/10NH$_4$NO$_3$, *b* 80agar/20NH$_4$NO$_3$, *c* 70agar/30NH$_4$NO$_3$, *d* 60agar/40NH$_4$NO$_3$ *e* 50agar/50NH$_4$NO$_3$, *f* 40agar/60NH$_4$NO$_3$, *g* 30agar/70NH$_4$NO$_3$ BPEs
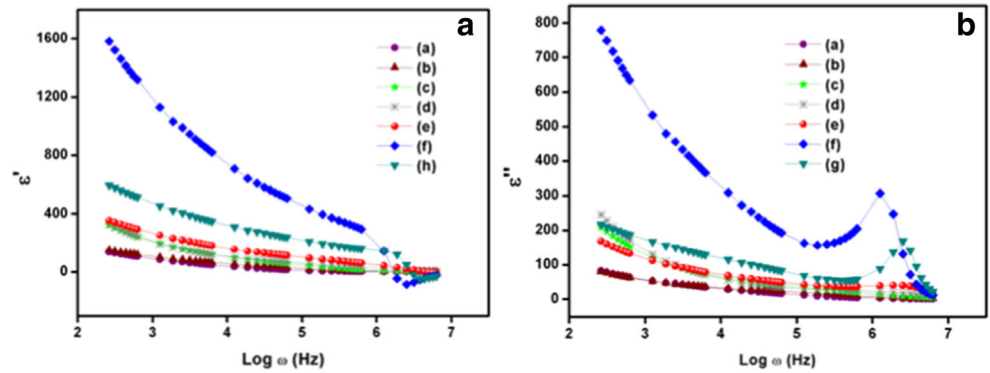
gives dc conductivity (σ_{dc}) of polymer complex, and the high-frequency region corresponds to the bulk relaxation phenomenon, which is due to the coulombic interaction of charge carrier and disorder within the structure [38]. From the plot in Fig. 6, it can be observed that the spectra consist of two well-defined regions, low-frequency dispersive region due to electrode polarization effects and the plateau region representing the DC conductivity. At low frequencies, the ionic conductivity is high enough to produce a significant build-up of charges at the electrodes which reduces the effective applied field and hence the conductivity. At higher frequency range, the period of the applied field is too short for the charging to occur, and the ac conductivity is generally taken as frequency-independent value, which is equal to the dc conduction [34].

Dielectric analysis

Dielectric constant is representative of stored charge in a material while dielectric loss is a measure of energy losses to move ions when the polarity of electric field reverses rapidly [39]. The dielectric behaviour of any polymeric system may be described by the complex permittivity, ϵ^*, which is defined by the relation,

$$\varepsilon^* = \varepsilon'(\omega) - j\varepsilon''(\omega) = -j/\omega\, C_0 Z^* \tag{3}$$

where the real $\varepsilon'(\omega)$ and imaginary $\varepsilon''(\omega)$ components are the storage (dielectric constant) and loss of energy (dielectric loss)

in each cycle of the applied electric field [40], Z^* is the complex impedance, C_0 is the vacuum capacitance and ω is the angular frequency of the applied electric field.

Figure 7a, b represents the frequency dependence of ε' and ε'' for all the prepared polymer electrolytes with different compositions of ammonium nitrate salt. No relaxation peaks are observed in Fig. 7a indicating that the increase in conductivity is mainly due to the increase in number density of mobile ions. On the other hand, in Fig. 7b, a peak has been observed at the high-frequency region for the 40agar/60NH₄NO₃ and 30agar/70NH₄NO₃ polymer complex which indicates that the peak formed is α-relaxation peak caused by main chain dipoles [41]. The decreasing ε' and ε'' with increasing frequency is attributed to the tendency of the dipoles in the polymer chains to orient themselves in the direction of the applied electric field [36]. Towards higher frequencies, the fast periodic reversal of the electric field occurs; hence, the polarization due to charge accumulation decreases at the electrode–electrolyte interface, which in turn contributes to the decrease in ε' and ε'' [42]. Dielectric results imply that the electrolyte systems in the present work confirm the non-Debye behaviour.

Modulus analysis

Generally, the electrical modulus spectrum is used to study the ion transport process of ionic conductors. Figure 8a, b represent

Fig. 8 **a**, **b** Frequency dependence of M′ and M″ of *a* 90agar/10NH$_4$NO$_3$, *b* 80agar/20NH$_4$NO$_3$, *c* 70agar/30NH$_4$NO$_3$, *d* 60agar/40NH$_4$NO$_3$, *e* 50agar/50NH$_4$NO$_3$, *f* 40agar/60NH$_4$NO$_3$, *g* 30agar/70NH$_4$NO$_3$ BPEs
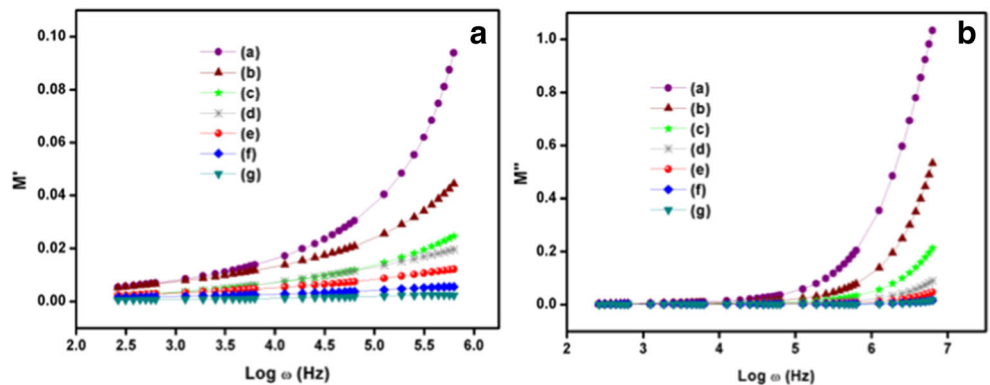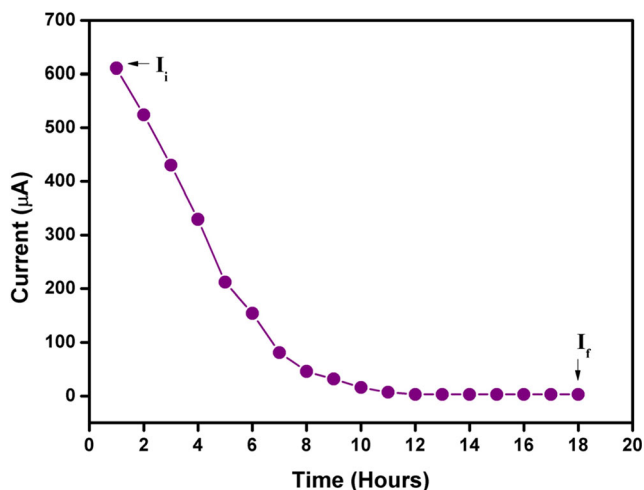
Fig. 9 Polarization current Vs time plot for 40agar/60NH$_4$NO$_3$

the frequency dependence of M′(ω) and M″(ω) at room temperature. Both M′ and M″ are observed to increase in the high-frequency end. At low frequencies, the of M′(ω) and M″(ω) decreases, which is due to the electrode polarization phenomenon and makes a negligible contribution. For all agar/NH$_4$NO$_3$ complex, the modulus value gradually increases with increase of frequencies, which is due to bulk effect. The plot that shows long tails at low frequencies are due to their large capacitance values associated with electrodes. This further confirms the non-Debye behaviour in the samples [42].

Transference number measurement

The Wagner's polarization method is used to calculate the transference number of the blend polymer electrolyte corresponding to ionic (t$_{ion}$) and electronic (t$_{ele}$) transport number [43]. The transference numbers are calculated using the following equations:

$$t_+ = (I_i - I_f)/I_i \quad (4)$$

$$t_- = I_f/I_i \quad (5)$$

where I$_i$ is the initial current and I$_f$ is the final residual current. To measure the total charge transport number, aluminium blocking electrodes are used to hold the polymer electrolyte samples. The DC current is monitored as a function of time on the application of a fixed DC bias voltage of 1.65 V. Figure 9 shows the plot of DC polarization current versus time for 40agar/60 NH$_4$NO$_3$ polymer complex. Initially, the

polarization current decreases with time, which happens when the ions migrate due to the applied field balanced by diffusion and hence leads to the cell polarization.

The value of ionic transference (t$_{ion}$) number for the highest conducting polymer electrolyte film 40agar/60NH$_4$NO$_3$ was found to be 0.99. This suggests that the charge transport in this polymer electrolyte was primarily due to ions, which are close to unity and only a negligible contribution comes from the electron. The diffusion coefficients of cations and anions of 50agar/50NH$_4$NO$_3$, 40agar/60NH$_4$NO$_3$ and 30agar/70NH$_4$NO$_3$ were calculated using the following equations [44], which are listed in Table 4:

$$D_+ + D_- = (kT\sigma/ne^2) \quad (6)$$

$$t_+ = D_+/(D_+ + D_-) \quad (7)$$

The ionic mobility of cations and anions of polymer electrolytes have been calculated using the following equations:

$$\mu = \mu_+ + \mu_- = \sigma/ne \quad (8)$$

$$t_+ = \mu_+/(\mu_+ + \mu_-) \quad (9)$$

where e is the charge of the electron; k Boltzmann constant; T absolute temperature; n is the number of charge carriers stochiometrically related to the salt composition; μ_+ and μ_- are the ionic mobility of cation and anion, respectively and D$_+$ and D$_-$ is the diffusion coefficients of cation and anion, respectively. It can be seen from the table that the number of density of mobile ions increases as conductivity increases. This further confirms that conductivity is actually controlled by the number of mobile ions in the samples.

Construction of single-PEM fuel cell

The cell consists of bipolar graphite plates with parallel flow channel area of 7.84 cm^2 and mounted on the two base plates, which is made up of acrylic. A silicon gasket is placed between the two graphite plates. The positive electrode (cathode) and negative electrode (anode) made up of carbon cloth of area ~8.41 cm^2, which are coated with Pt at a uniform rate of 0.15 mg/cm^2. The Pt-coated carbon cloth (electrodes) which acts as catalyst layer is kept on the either side of flow channel. The highest proton-conducting membrane 40agar/60NH$_4$NO$_3$ is

Table 4 Transport parameters

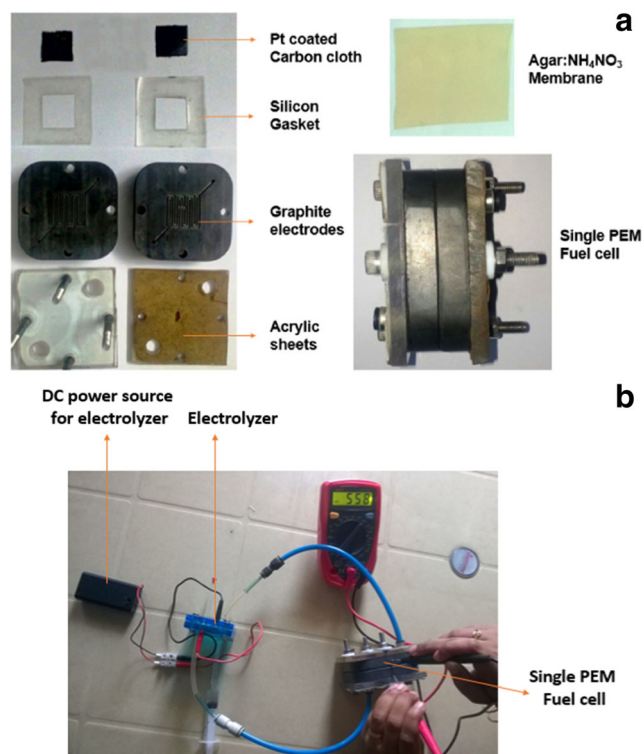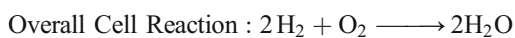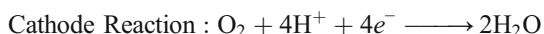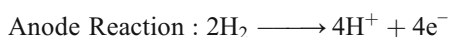| Composition (mol%)	N (cm^{-3})	t$_{ion}$	D$_+$ (cm^2 s^{-1})	D$_-$ (cm^2 s^{-1})	μ_+ (cm^2 V^{-1} s^{-1})	μ_- (cm^2 V^{-1} s^{-1})
50agar/50NH$_4$NO$_3$	6.47×10^{21}	0.98	4.7×10^{-9}	6.8×10^{-11}	1.8×10^{-7}	2.6×10^{-9}
40agar/60NH$_4$NO$_3$	7.76×10^{21}	0.99	1.4×10^{-8}	1.1×10^{-10}	5.2×10^{-7}	4.3×10^{-9}
30agar/70NH$_4$NO$_3$	9.05×10^{21}	0.98	8.1×10^{-9}	8.8×10^{-11}	3.1×10^{-7}	3.4×10^{-9}

Fig. 10 a Single PEM Fuel cell and its components. **b** Open circuit voltage of single PEM fuel cell

sandwiched between the two electrodes. The single-PEM fuel cell has been assembled with the above mentioned configuration and is shown in Fig. 10a. Using a small electrolyser operated by a voltage of 3 V is used to produce hydrogen and oxygen gas separately. The hydrogen gas with flow rate of 10 ml/min and oxygen gas at a rate of 8 ml/min are passed through the single fuel cell. The anode and the cathode reaction for a PEM fuel cell are given in below equations:

$$\text{Anode Reaction}: 2H_2 \longrightarrow 4H^+ + 4e^-$$

$$\text{Cathode Reaction}: O_2 + 4H^+ + 4e^- \longrightarrow 2H_2O$$

$$\text{Overall Cell Reaction}: 2H_2 + O_2 \longrightarrow 2H_2O$$

Standard Nafion 117 membrane is placed in constructed fuel cell and a voltage of 900 mV is obtained. Afterwards, the highest conducting polymer membrane 40agar/60NH$_4$NO$_3$ is placed in fuel cell kit and a voltage of 558 mV is observed and it is shown in Fig. 10b.

Conclusion

In this work, a novel, biodegradable and high proton-conducting polymer electrolyte based on agar/NH$_4$NO$_3$ was prepared by the method of solution casting. XRD analysis

suggested an increase in the amorphous nature with increase in NH4NO$_3$ salt concentrations in the polymer matrix. FTIR study confirms the complexation of the polymer with the dopant salt. The temperature dependence of ionic conductivity follows the Arrhenius relation. The highest conductivity 6.57×10^{-4} was achieved for the 40agar/60NH$_4$NO$_3$ polymer electrolyte with lowest activation energy 0.12 eV. Transference number data show that the conductivity mainly arises due to ions rather than electrons. Thus, the optimized polymer electrolyte 40agar/60NH$_4$NO$_3$ with high conductivity was used for the construction of single-PEM fuel cell, and the OCV was found to be 556 mV. All these results suggest that the polymer complex of agar doped with ammonium salts, which is cheap and biodegradable, are very attractive for electrochemical device applications such as fuel cells and batteries.

References

1. Smitha B, Sridhar S, Khan A (2005) Solid polymer electrolyte membranes for fuel cell applications—a review. J Membr Sci 259:10–26
2. Casciola M, Alberti G, Sganappa M, Narducci R (2006) On the decay of Nafion proton conductivity at high temperature and relative humidity. J Power Sources 162:141–145
3. Lu D, Xiao C, Xu S (2009) Starch-based completely biodegradable polymer materials. Express Polym Lett 3:366–375
4. Ponez L, Sentanin F, Majid S, Arof A, Pawlicka A (2012) Ion-conducting membranes based on gelatin and containing LiI/I$_2$ for electrochromic devices. Mol Cryst Liq Cryst 554:239–251
5. Aziz SB, Abidin Z, Arof A (2010) Effect of silver nanoparticles on the DC conductivity in chitosan–silver triflate polymer electrolyte. Phys B Condens Matter 405:4429–4433
6. Nik Aziz N, Idris N, Isa M (2010) Solid polymer electrolytes based on methylcellulose: FT-IR and ionic conductivity studies. Int J Polym Anal Charact 15:319–327
7. Araki C (1966) Some recent studies on the polysaccharides of agarophytes. Proc Fifth Int Seaweed Symp 5:3
8. Raphael E, Avellaneda CO, Manzolli B, Pawlicka A (2010) agar-based films for application as polymer electrolytes. Electrochim Acta 55:1455–1459
9. Moon WG, Kim GP, Lee M, Song HD, Yi J (2015) A biodegradable gel polymer electrolyte for use in high-performance flexible supercapacitors. ACS Applied Materials Interfaces 7(6):3503–3511
10. Koh JCH, Ahmad ZA, Mohamad AA (2012) Bacto agar-based polymer electrolyte. Ionics 18:359–364
11. Singh R, Jadhav NA, Majumder S, Bhattacharya B, Singh PK (2013) Novel biopolymer gel electrolytes for dye-sensitized solar cell application. Carbohydr Polym 91(2):682–685
12. Singh R, Singh PK, Tomar SK, Bhattacharya B (2016) Synthesis, characterization and dye-sensitized solar cell fabrication using solid polymer electrolyte membranes. High performance polymers 28(1):47–54
13. Alias SS, Mohamad AA (2013) Effect of NH$_4$I and I$_2$ concentration on agar gel polymer electrolyte properties for a dye-sensitized solar cell. Ionics 19:1185–1194
14. Boukamp BA (1986a) A nonlinear least squares fit procedure for analysis of immittance data of electrochemical systems. Solid State Ionics 20:31–44
15. Boukamp BA (1986b) A package for impedance/admittance data analysis. Solid State Ionics 18:136–140

16. Aji MP, Bijaksana S, Abdullah M (2012) A general formula for ion concentration-dependent electrical conductivities in polymer electrolytes. Am J Appl Sci 9:946

17. Shukur M, Kadir M (2015) Electrical and transport properties of NH4Br-doped corn starch-based solid biopolymer electrolyte. Ionics 21:111–124

18. Khiar AA, Arof A (2010) Conductivity studies of starch-based polymer electrolytes. Ionics 16:123–129

19. Appetecchi G, Romagnoli P, Scrosati B (2001) Composite gel membranes: a new class of improved polymer electrolytes for lithium batteries. Electrochem Commun 3:281–284

20. Appetecchi GB, Croce F, Romagnoli P, Scrosati B, Heider U, Oesten R (1999) High-performance gel-type lithium electrolyte membranes. Electrochem Commun 1:83–86

21. Lan Z, Wu J, Lin J, Huang M, Li P, Li Q (2008) Influence of ionic additives NaI/I 2 on the properties of polymer gel electrolyte and performance of quasi-solid-state dye-sensitized solar cells. Electrochim Acta 53:2296–2301

22. Chirapart A, Ohno M, Ukeda H, Sawamura M, Kusunose H (1995) Chemical composition of agars from a newly reported Japanese agarophyte, Gracilariopsis lemaneiformis. J Appl Phycol 7(4):359–365

23. Armisen R, Galatas F (1987) Production, properties and uses of agar. Production and utilization of products from commercial seaweeds FAO Fish Tech Pap 288:1–57

24. Christiaen D, Bodard M (1983) Spectroscopie infrarouge de films d 'agar de *Gracilaria verrucosa* (Huds.) Papenfuss. Bot Mar 26:425–428

25. Rochas C, Lahaye M, Yaphe W (1986) Sulfate content of carrageenan and agar determined by infrared spectroscopy. Bot Mar 29: 335–340

26. El-Hefian EA, Nasef MM, Yahaya AH (2012) Preparation and characterization of chitosan/agar blended films: part 1. Chemical structure and morphology. Journal of Chemistry 9:1431–1439

27. Leones R, Sentanin F, Rodrigues L, Marrucho I, Esperança J, Pawlicka A, Silva M (2012) Investigation of polymer electrolytes based on agar and ionic liquids. Express Polym Lett 6:1007

28. Ramesh S, Liew C-W, Arof A (2011) Ion conducting corn starch biopolymer electrolytes doped with ionic liquid 1-butyl-3-methylimidazolium hexafluorophosphate. J Non-Cryst Solids 357: 3654–3660

29. Ahmad N, Isa M (2016) Characterization of un-plasticized and propylene carbonate plasticized carboxymethyl cellulose doped ammonium chloride solid biopolymer electrolytes. Carbohydr Polym 137:426–432

30. Sikkanthar S, Karthikeyan S, Selvasekarapandian S, Pandi DV, Nithya S, Sanjeeviraja C (2015) Electrical conductivity characterization of polyacrylonitrile-ammonium bromide polymer electrolyte system. J Solid State Electrochem 19:987–999

31. Shamsudin I, Ahmad A, Hassan NH, Kaddami H (2016) Biopolymer electrolytes based on carboxymethyl K-carrageenan and imidazolium ionic liquid. Ionics:1–11

32. Rajeswari N, Selvasekarapandian S, Sanjeeviraja C, Kawamura J, Bahadur SA (2014) A study on polymer blend electrolyte based on PVA/PVP with proton salt. Polym Bull 71:1061–1080

33. Monisha S, Selvasekarapandian S, Mathavan T, Benial AMF, Manoharan S, Karthikeyan S (2016) Preparation and characterization of biopolymer electrolyte based on cellulose acetate for potential applications in energy storage devices. J Mater Sci Mater Electron 27(9):9314–9324

34. Ramya C, Selvasekarapandian S, Savitha T, Hirankumar G, Baskaran R, Bhuvaneswari M, Angelo P (2006) Conductivity and thermal behavior of proton conducting polymer electrolyte based on poly (N-vinyl pyrrolidone). Eur Polym J 42:2672–2677

35. Chai M, Isa M (2013) Electrical characterization and ionic transport properties of carboxyl methylcellulose-oleic acid solid polymer electrolytes. Int J Polym Anal Charact 18:280–286

36. Nithya H, Selvasekarapandian S, Kumar DA, Sakunthala A, Hema M, Christopherselvin P, Kawamura J, Baskaran R, Sanjeeviraja C (2011) Thermal and dielectric studies of polymer electrolyte based on P (ECH-EO). Mater Chem Phys 126:404–408

37. Kopitzke RW, Linkous CA, Anderson HR, Nelson GL (2000) Conductivity and water uptake of aromatic-based proton exchange membrane electrolytes. J Electrochem Soc 147:1677–1681

38. Kim C, Lee G, Liou K, Ryu KS, Kang S-G, Chang SH (1999) Polymer electrolytes prepared by polymerizing mixtures of polymerizable PEO-oligomers, copolymer of PVDC and poly (acrylonitrile), and lithium triflate. Solid State Ionics 123:251–257

39. Woo H, Majid S, Arof A (2012) Dielectric properties and morphology of polymer electrolyte based on poly (ε-caprolactone) and ammonium thiocyanate. Mater Chem Phys 134:755–761

40. Dutta P, Biswas S, De SK (2002) Dielectric relaxation in polyaniline–polyvinyl alcohol composites. Mater Res Bull 37:193–200

41. Sivadevi S, Selvasekarapandian S, Karthikeyan S, Sanjeeviraja C, Nithya H, Iwai Y, Kawamura J (2015) Proton-conducting polymer electrolyte based on PVA-PAN blend doped with ammonium thiocyanate. Ionics 21:1017–1029

42. Ramesh S, Yahaya A, Arof A (2002) Dielectric behaviour of PVC-based polymer electrolytes. Solid State Ionics 152:291–294

43. Wagner JB, Wagner C (1957) Electrical conductivity measurements on cuprous halides. J Chem Phys 26:1597–1601

44. Chandra S (1981) Superionic solids: principles and applications. North-Holland Publishing Co., Amsterdam. xi + 404, 22 × 15 cm, illustrated